

Research Article

Some Thiophene Derivatives as Corrosion Inhibitors for Carbon Steel in Hydrochloric Acid

A. S. Fouda,¹ A. A. Attia,² and A. A. Negm³

¹ Department of Chemistry, Faculty of Science, Mansoura University, El-Mansoura, Egypt

² Department of Chemistry, Faculty of Science, Zagazig University, Zagazig, Egypt

³ East Delta Electricity Production Company, Damietta, Egypt

Correspondence should be addressed to A. S. Fouda; asfouda@mans.edu.eg

Received 24 September 2013; Revised 12 December 2013; Accepted 18 February 2014; Published 7 May 2014

Academic Editor: Elena V. Pereloma

Copyright © 2014 A. S. Fouda et al. This is an open access article distributed under the Creative Commons Attribution License, which permits unrestricted use, distribution, and reproduction in any medium, provided the original work is properly cited.

Corrosion inhibitive performance of some thiophene derivatives during the acidic corrosion of carbon steel surface in 1 M HCl was investigated by chemical technique (weight loss) and electrochemical techniques (potentiodynamic polarization, electrochemical frequency modulation, and electrochemical impedance spectroscopy). The effect of temperature on the corrosion rate was investigated by the weight loss method, and some thermodynamic parameters for corrosion and adsorption processes were determined and discussed. The results show that the inhibition efficiency increased with the increase in inhibitor concentration and temperature. The adsorption of thiophene derivatives on the carbon steel surface obeys Langmuir adsorption isotherm. The obtained results indicated that the investigated compounds are chemically adsorbed on the steel surface. Potentiodynamic polarization studies showed that these compounds are mixed-type inhibitors and the results obtained from the techniques are in good agreement.

1. Introduction

Carbon steel has remarkable economic and attractive materials for engineering applications owing to its low cost, easy availability, and high mechanical strength. The use of inhibitors is one of the most practical methods to protect metals against acid attack. The most widely used acid inhibitors are organic compounds containing oxygen, nitrogen, and/or sulfur [1–5]. Acid inhibitors have many important roles in the industrial field such as a component in pretreatment composition, cleaning solutions, and in acidification of oil wells. Heteroatoms as sulfur, nitrogen, and oxygen as well as aromatic rings in their structure are the major adsorption centers. Some works have studied the influence of organic compounds containing nitrogen on the corrosion resistance of steel in acidic media [6–18] most organic inhibitors decrease corrosion rate by adsorption on the metal surface. To be effective, an inhibitor must also displace water from the metals surface to block active corrosion sites and interact with the anodic or cathodic reaction sites to retard the oxidation and/or reduction of corrosion reaction. So, the inhibition

efficiency of organic compounds depends on the structure of the inhibitor, the characteristics of the environment, and so forth. Several organic compounds have been evaluated as corrosion inhibitors for carbon steel in acidic media, so the aim of this work is to study the inhibition properties of some thiophene derivatives for the corrosion of 1018 carbon steel in 1 M HCl. The main techniques were employed: chemical (weight loss) and electrochemical ones (potentiodynamic, electrochemical frequency modulation, EFM, and electrochemical impedance spectroscopy, EIS). These techniques were performed in 1 M HCl without and with the presence of the investigated compounds in the concentration range (0 to 12×10^{-5} M).

2. Methods

2.1. Materials. Rectangular specimens with dimensions $2 \times 2 \times 0.2$ cm of carbon steel that is chemical composition can be seen from Table 1. It was used for weight loss measurements. For electrochemical tests, the exposed surface area of metal was 1.00 cm^2 .

TABLE 1: Chemical composition (weight %) of the carbon steel.

Element	C	Mn	P	Si	Fe
Weight (%)	0.2	0.35	0.024	0.003	Rest

2.2. *Inhibitors.* Thiophene derivatives were prepared as reported before [19]. Table 2 shows the structures, names, molecular weights, and molecular formulas of these compounds.

2.3. *Solutions.* Hydrochloric acid (37%), ethyl alcohol, and acetone were BDH grades and purchased from Algamhoria Co. (Egypt). Bidistilled water was used for preparing test solutions for all measurements.

2.4. Procedures Used for Corrosion Measurements

2.4.1. *Weight Loss Tests.* Medium carbon steel specimens were mechanically abraded up to 1200 grades emery paper and degreased with acetone, rinsed with bidistilled water two times, and finally dried between filter paper. After weighting accurately, the specimens were immersed in 100 mL of 1M HCl with and without different concentrations of thiophene derivatives. After different immersion times (30, 60, 90, 120, 150, and 180 min) the carbon steel samples were taken out, washed with bidistilled water, dried, and weighted accurately. The experiments were done in triplicate and the average value of the weight loss was taken. The average weight loss of the three parallel carbon steel sheets could be obtained at required temperature. The inhibition efficiency (%IE) and the degree of surface coverage (θ) of the investigated inhibitors on the corrosion of carbon steel were calculated as follows [20]:

$$\text{IE}\% = \theta \times 100 = \left[\frac{(W_0 - W)}{W_0} \right] \times 100, \quad (1)$$

where W_0 and W are the values of the average weight loss in the absence and presence of the inhibitor, respectively.

2.4.2. *Potentiodynamic Polarization Measurements.* Polarization experiments were carried out in a conventional three-electrode cell with platinum gauze as the auxiliary electrode and a saturated calomel electrode (SCE) coupled to a fine Luggin capillary as reference electrode. The working electrode was in the form of a square cut from copper sheet of equal composition embedded in epoxy resin of polytetrafluoroethylene so that the flat surface area was 1 cm^2 . Prior to each measurement, the electrode surface was pretreated in the same manner as the weight loss experiments. Before measurements, the electrode was immersed in solution for 30 min. until a steady state was reached. The potential was started from -600 to $+400$ mV versus open circuit potential (Eocp). All experiments were carried out in freshly prepared solutions at 25°C and results were always repeated at least three times to check the reproducibility.

2.4.3. *Electrochemical Impedance Spectroscopy Measurements.* Impedance measurements were carried out using AC signals

of 5 mV peak to peak amplitude at the open circuit potential in the frequency range of 100 kHz to 0.1 Hz. All impedance data were fitted to appropriate equivalent circuit using the Gamry Echem Analyst software.

2.4.4. *Electrochemical Frequency Modulation Technique.* EFM experiments were performed with applying potential perturbation signal with amplitude 10 mV with two sine waves of 2 and 5 Hz. The choice for the frequencies of 2 and 5 Hz was based on three arguments [21–23]. The larger peaks were used to calculate the corrosion current density ($i_{\text{corr.}}$), the Tafel slopes (β_c and β_a), and the causality factors CF-2 and CF-3 [24].

All electrochemical experiments were carried out using Gamry instrument PCI300/4 Potentiostat/Galvanostat/Zra analyzer, DCI05 corrosion software, EIS300 electrochemical impedance spectroscopy software, EFM140 electrochemical frequency modulation software, and Echem Analyst 5.5 for results plotting, graphing, data fitting, and calculating.

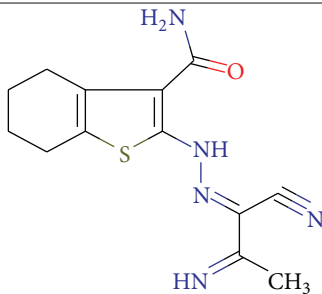
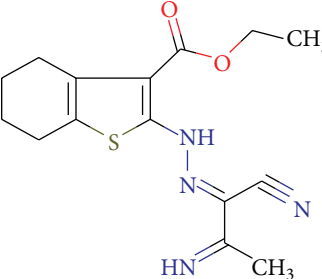
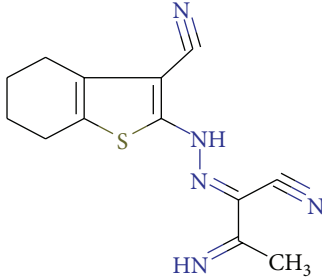
3. Results and Discussion

3.1. *Weight Loss Measurements.* Weight loss of carbon steel was determined, at various time intervals, in the absence and presence of different concentrations of thiophene derivatives compounds (A, B, and C). The obtained weight loss time curves are represented in Figure 1 for inhibitor (A), the most effective one. Similar curves were obtained for other inhibitors (not shown). The inhibition efficiency of corrosion was found to be dependent on the inhibitor concentration. The curves obtained in the presence of inhibitors fall significantly below that of free acid. In all cases, the increase in the inhibitor concentration was accompanied by a decrease in weight loss and an increase in the percentage inhibition. These results lead to the conclusion that the compounds under investigation are fairly efficient as inhibitors for carbon steel dissolution in hydrochloric acid solution. Also, the degree of surface coverage (θ) by the inhibitor, calculated from (1), would increase by increasing the inhibitor concentration. In order to get a comparative view, the variation of the percentage inhibition (%IE) of the three inhibitors with their molar concentrations was calculated according to (2). The values obtained are summarized in Table 3. Careful inspection of these results showed that, at the same inhibitor concentration, the order of inhibition efficiencies is as follows: $A > B > C$.

3.1.1. *Adsorption Isotherm.* One of the most convenient ways of expressing adsorption quantitatively is by deriving the adsorption isotherm that characterizes the metal/inhibitor/environment system. Various adsorption isotherms were applied to fit θ values, but the best fit was found to obey Langmuir adsorption isotherm that are represented in Figures 2, 3, and 4 for inhibitors (A), (B), and (C), respectively; Langmuir adsorption isotherm may be expressed by the following:

$$\frac{C}{\theta} = \left(\frac{1}{K} \right) + C, \quad (2)$$

TABLE 2: Chemical structure of inhibitors.

Inhibitor	Structures	Names	Mol.Wt., Mol. formulas
A		2-[(2Z)-2-(1-cyano-2-iminopropylidene)hydrazinyl]-4,5,6,7-tetrahydro-1-benzothiophene-3-carboxamide	289.35 C ₁₃ H ₁₅ N ₅ OS
B		ethyl 2-[(2Z)-2-(1-cyano-2-iminopropylidene)hydrazinyl]-4,5,6,7-tetrahydro-1-benzothiophene-3-carboxylate	318.39 C ₁₅ H ₁₈ N ₄ O ₂ S
C		2-[(2Z)-2-(1-cyano-2-iminopropylidene)hydrazinyl]-4,5,6,7-tetrahydro-1-benzothiophene-3-carbonitrile	271.34082 C ₁₃ H ₁₃ N ₅ S

where C is the concentration (mol L^{-1}) of the inhibitor in the bulk electrolyte, θ is the degree of surface coverage ($\theta = \%IE/100$), and K_{ads} is the adsorption equilibrium constant. A plot of C/θ versus C should give straight lines with slope equal to unity and the intercept is $(1/K_{\text{ads}})$. In order to get a comparative view, the variation of the adsorption equilibrium constant (K_{ads}) of the inhibitors with their molar concentrations was calculated according to (3). The experimental data give good curves fitting for the applied adsorption isotherm as the correlation coefficients (R^2) were in the range (0.943–0.999). The values obtained are given in Table 4.

These results confirm the assumption that these compounds are adsorbed on the metal surface through the protonated (N, S, and O) atoms or via the lone pair of electrons of (N, S, and O) atoms. The extent of inhibition is directly related to the performance of adsorption layer which is a sensitive function of the molecular structure. The equilibrium constant of adsorption K_{ads} obtained from the intercepts of Langmuir adsorption isotherm is related to the free energy of adsorption $\Delta G_{\text{ads}}^\circ$ as follows:

$$K_{\text{ads}} = \frac{1}{55.5} \exp \left[\frac{-\Delta G_{\text{ads}}^\circ}{RT} \right], \quad (3)$$

where 55.5 is the molar concentration of water in the solution in M^{-1} .

Plot of $(\Delta G_{\text{ads}}^\circ)$ versus T (Figure 5) gave the heat of adsorption ($\Delta H_{\text{ads}}^\circ$) and the standard entropy ($\Delta S_{\text{ads}}^\circ$) according to the thermodynamic basic equation (4) as follows:

$$\Delta G_{\text{ads}}^\circ = \Delta H_{\text{ads}}^\circ - T\Delta S_{\text{ads}}^\circ. \quad (4)$$

Table 5 clearly shows a good dependence of $\Delta G_{\text{ads}}^\circ$ on T , indicating the good correlation among thermodynamic parameters. The negative value of $\Delta G_{\text{ads}}^\circ$ ensures the spontaneity of the adsorption process and stability of the adsorbed layer on the steel surface. Generally, values of $\Delta G_{\text{ads}}^\circ$ around -20 kJ mol^{-1} or lower are consistent with the electrostatic interaction between the charged molecules and the charged metal (physisorption); those around -40 kJ mol^{-1} or higher involve charge sharing or transfer from organic molecules to the metal surface to form a coordinate type of bond (chemisorption) [25]. The calculated $\Delta G_{\text{ads}}^\circ$ values are closer to -40 kJ mol^{-1} indicating that the adsorption mechanism of the inhibitors on steel in 1M HCl solutions was typical of chemisorption. The unshared electron pairs in sulphur and nitrogen as well as in oxygen may interact with d-orbitals of steel to provide a protective chemisorbed film [26].

TABLE 3: Values of inhibition efficiencies (%IE) and surface coverage (θ) of inhibitors for the corrosion of carbon steel in 1 M HCl from weight loss measurements at different concentrations and at 25°C.

$C_{inh.} \times 10^{-5}$ (M)	A		B		C	
	%IE	θ	%IE	θ	%IE	θ
2	46.1	0.461	35.6	0.356	23.9	0.239
4	54.3	0.543	47.9	0.479	33.8	0.338
6	58.9	0.589	54.3	0.543	41.7	0.417
8	64.3	0.643	60.8	0.608	50.2	0.502
10	66	0.66	62.5	0.625	56.7	0.567
12	72.5	0.725	66.6	0.666	64.9	0.649

TABLE 4: Adsorption parameters for inhibitors in 1 M HCl obtained from Langmuir adsorption isotherm at different temperatures.

Temperature (°C)	A			B			C		
	$K_{ads} \times 10^{-3}$ (M ⁻¹)	Slope	R ²	$K_{ads} \times 10^{-3}$ (M ⁻¹)	Slope	R ²	$K_{ads} \times 10^{-3}$ (M ⁻¹)	Slope	R ²
25	42.82	1.24	0.988	30.01	1.24	0.988	13.37	1.00	0.943
35	36.87	1.13	0.985	43.23	1.19	0.985	14.87	1.02	0.957
45	57.13	1.04	0.987	58.75	1.12	0.997	16.46	1.03	0.964
55	139.41	1.05	0.999	57.13	1.00	0.999	45.99	1.08	0.995

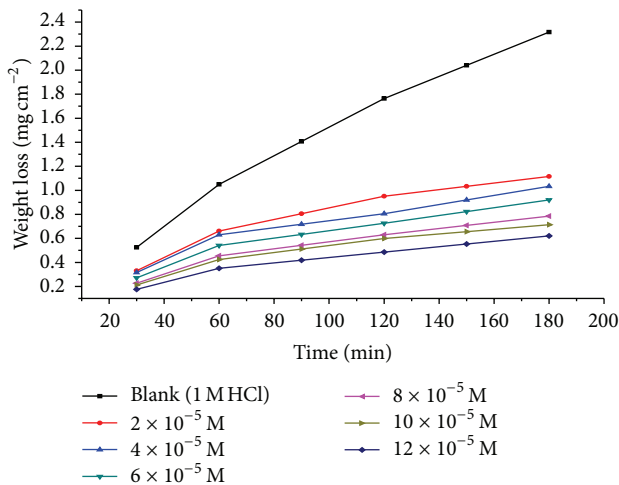


FIGURE 1: Weight loss time curves for the corrosion of carbon steel in 1 M HCl in the absence and presence of different concentrations of inhibitor (A) at 25°C.

The values of thermodynamic parameter for the adsorption of inhibitors (Table 5) can provide valuable information about the mechanism of corrosion inhibition. While an endothermic adsorption process ($\Delta H_{ads}^{\circ} > 0$) is attributed unequivocally to chemisorption [27], an exothermic adsorption process ($\Delta H_{ads}^{\circ} < 0$) may involve either physisorption or chemisorption or mixture of both processes. The ΔS_{ads}° values in the presence of inhibitors in 1 M HCl are positive. This indicates that an increase in disorder takes place from reactants to the metal-adsorbed reaction complex [28].

3.1.2. Effect of Temperature. The effect of temperature on the corrosion rate of carbon steel in 1 M HCl and in presence

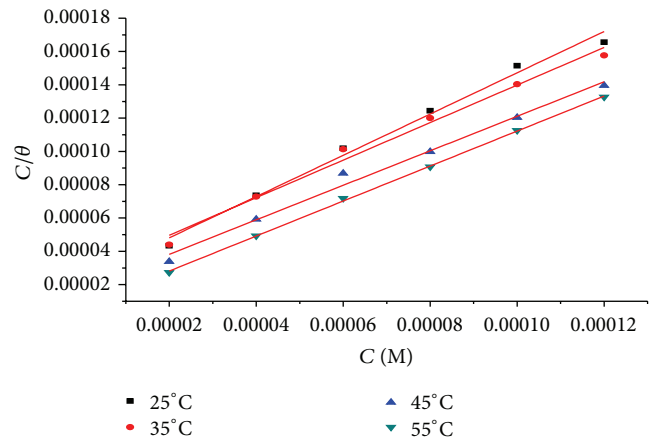


FIGURE 2: Langmuir adsorption isotherm of inhibitor (A) on carbon steel surface in 1 M HCl at different temperatures.

of different inhibitors concentrations was studied in the temperature range of 298–328 K using weight loss measurements. Similar curves were obtained for other inhibitors (not shown). As the temperature increases, the rate of corrosion increases; nevertheless, the inhibition efficiency of the additives increases as shown in Table 6 for inhibitor (A), the most effective one. Similar tables were obtained for other inhibitors (not shown). Table 6 illustrates that the adsorption is aided by increasing the temperature. This behavior proves that the adsorption of inhibitors on carbon steel surface occurs through chemical adsorption. Ivanov [29] considers the increase of %IE with increasing the temperature as the change in the nature of the adsorption mode; the inhibitor is being physically adsorbed at lower temperatures, while chemisorption is favored as temperature increases. Similar observations were reported by other authors [30–32].

TABLE 5: Thermodynamic parameters for the adsorption of inhibitors on carbon steel surface in 1 M HCl at different temperatures.

Inhibitor	Temperature (°C)	$K_{\text{ads.}} \times 10^{-3}$ (M^{-1})	$-\Delta G_{\text{ads.}}^{\circ}$ (kJ mol^{-1})	$\Delta H_{\text{ads.}}^{\circ}$ (kJ mol^{-1})	$\Delta S_{\text{ads.}}^{\circ}$ (kJ mol^{-1})
A	25	42.8	36.4	2.8	0.13
	35	36.9	37.2		0.12
	45	57.1	39.6		0.12
	55	139.4	43.3		0.13
B	25	30	35.5	1.7	0.12
	35	43.2	37.6		0.12
	45	58.8	39.7		0.12
	55	57.1	40.8		0.12
C	25	13.4	33.5	3	0.12
	35	14.9	34.9		0.11
	45	16.5	36.3		0.11
	55	46	40.2		0.12

TABLE 6: Values of inhibition efficiencies %IE, coverage factor (θ), and corrosion rate (C.R.) of inhibitor (A) for the corrosion of carbon steel in 1 M HCl from weight loss measurements at different concentrations at temperature range of 298–328 K.

Concentration $\times 10^{-5}$ (M)	298 K			308 K			318 K			328 K		
	θ	%IE	C.R.	θ	%IE	C.R.	θ	%IE	C.R.	θ	%IE	C.R.
2	0.461	46.1	0.008	0.454	45.4	0.014	0.589	58.9	0.03	0.732	73.2	0.03
4	0.543	54.3	0.007	0.549	54.9	0.012	0.675	67.5	0.02	0.813	81.3	0.02
6	0.589	58.9	0.006	0.593	59.3	0.011	0.69.1	69.1	0.02	0.835	83.5	0.02
8	0.643	64.3	0.005	0.67	66.66	0.009	0.801	80.1	0.01	0.882	88.2	0.01
10	0.66	66	0.005	0.712	71.2	0.008	0.83	83	0.01	0.889	88.9	0.01
12	0.725	72.5	0.004	0.761	76.1	0.006	0.86	86	0.01	0.905	90.5	0.01

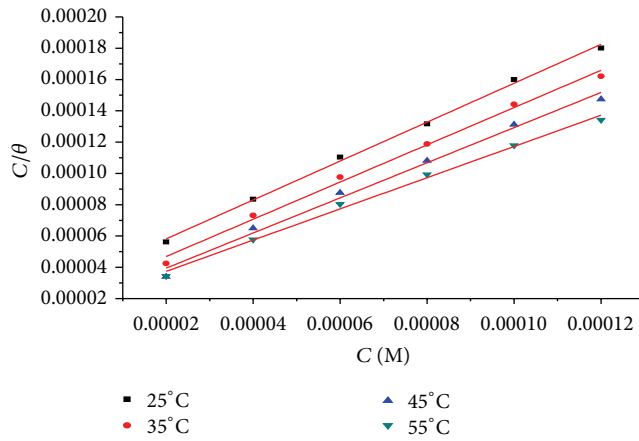


FIGURE 3: Langmuir adsorption isotherm of inhibitor (B) on carbon steel surface in 1 M HCl at different temperatures.

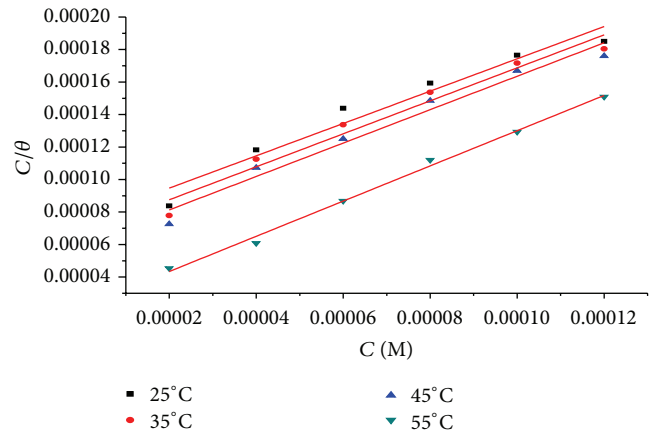


FIGURE 4: Langmuir adsorption isotherm of inhibitor (C) on carbon steel surface in 1 M HCl at different temperatures.

3.1.3. *Kinetic-Thermodynamic Corrosion Parameter.* The activation parameters for the corrosion process were calculated from Arrhenius-type plot according to (5) as follows:

$$k_{\text{corr.}} = A \exp\left(\frac{E_a^*}{RT}\right), \quad (5)$$

where E_a^* is the apparent activation corrosion energy, R is the universal gas constant, T is the absolute temperature,

and A is the Arrhenius preexponential constant. Values of apparent activation energy of corrosion (E_a^*) for carbon steel in 1 M HCl shown in Table 7 without and with various concentrations of compound (A) determined from the slope of $\log(k_{\text{corr.}})$ versus $1/T$ plots are shown in Figure 6. Inspection of the data shows that the activation energy is lower in the presence of inhibitors than in its absence. This was attributed to the slow rate of inhibitor adsorption with a resultant closer

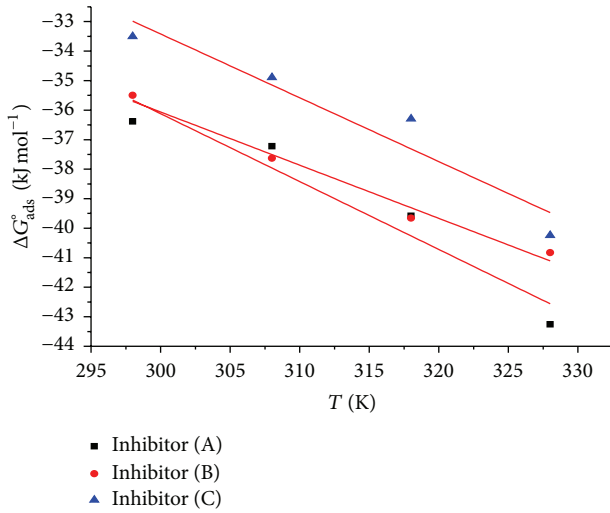


FIGURE 5: Variation of $\Delta G_{\text{ads}}^{\circ}$ versus T for the adsorption of inhibitors on carbon steel surface in 1 M HCl at different temperatures.

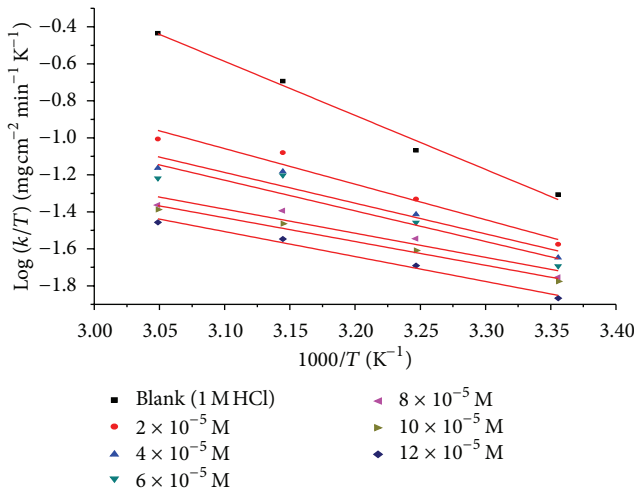


FIGURE 6: $\log(k)$ versus $(1/T)$ curves for Arrhenius plots for carbon steel corrosion rates ($k_{\text{corr.}}$) after 120 minutes of immersion in 1 M HCl in the absence and presence of various concentrations of inhibitor (A).

approach to equilibrium during the experiments at higher temperatures according to Hour and Holliday [33]. But Riggs and Hurd [34] explained that the decrease in the activation energy of corrosion at higher levels of inhibition arises from a shift of the net corrosion reaction from the uncovered part of the metal surface to the covered one. Schmid and Huang [35] found that organic molecules inhibit both the anodic and cathodic partial reactions on the electrode surface and a parallel reaction takes place on the covered area, but the reaction rate on the covered area is substantially less than that on uncovered area which is similar to the present study. The alternative formulation of transition state equation is shown in (6) as follows:

$$k_{\text{corr}} = \left(\frac{RT}{Nh} \right) \exp \left(\frac{\Delta S^*}{R} \right) \exp \left(-\frac{\Delta H^*}{RT} \right), \quad (6)$$

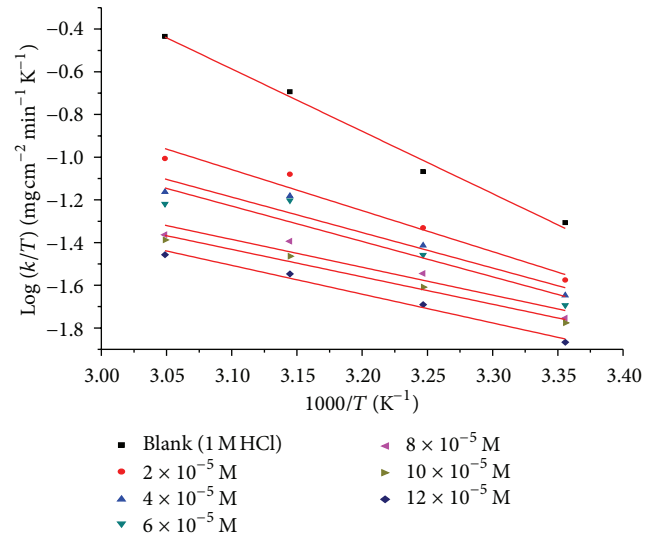


FIGURE 7: $\log(k/T)$ versus $(1/T)$ curves for Arrhenius plots for carbon steel corrosion rates ($k_{\text{corr.}}$) after 120 minutes of immersion in 1 M HCl in the absence and presence of various concentrations of inhibitor (A).

where $k_{\text{corr.}}$ is the rate of metal dissolution, h is Planck's constant, N is Avogadro's number, ΔS^* is the entropy of activation, and ΔH^* is the enthalpy of activation.

Figure 7 shows a plot of $(\log k/T)$ against $(1/T)$ in the case of inhibitor (A) in 1 M HCl. Similar behavior is observed in the case of inhibitors B and C (not shown). Straight lines are obtained with slopes equal to $(\Delta H^*/2.303R)$ and intercepts are $[\log(R/Nh) + \Delta S^*/2.303R]$ calculated in Table 7.

The decrease in E_a^* with the increase in inhibitor concentration (Table 7) is typical of chemisorption. The positive signs of the enthalpies (ΔH^*) reflect the endothermic nature of the steel dissolution process. Value of entropies (ΔS^*) implies that the activated complex at the rate determining step represents an association rather than a dissociation step, meaning that a decrease in disordering takes place from reactants toward the activated complex formation [30, 36]. However, the value of (ΔS^*) decreases gradually with increasing the inhibitor concentrations in all the acid media.

3.2. Electrochemical Measurements

3.2.1. *Electrochemical Frequency Modulation Technique (EFM)*. EFM is a nondestructive corrosion measurement technique that can directly and quickly determine the corrosion current values without prior knowledge of Tafel slopes and with only a small polarizing signal. These advantages of EFM technique make it an ideal candidate for online corrosion monitoring [37]. The great strength of the EFM is the causality factors which serve as an internal check on the validity of EFM measurement. The causality factors CF-2 and CF-3 are calculated from the frequency spectrum of the current responses.

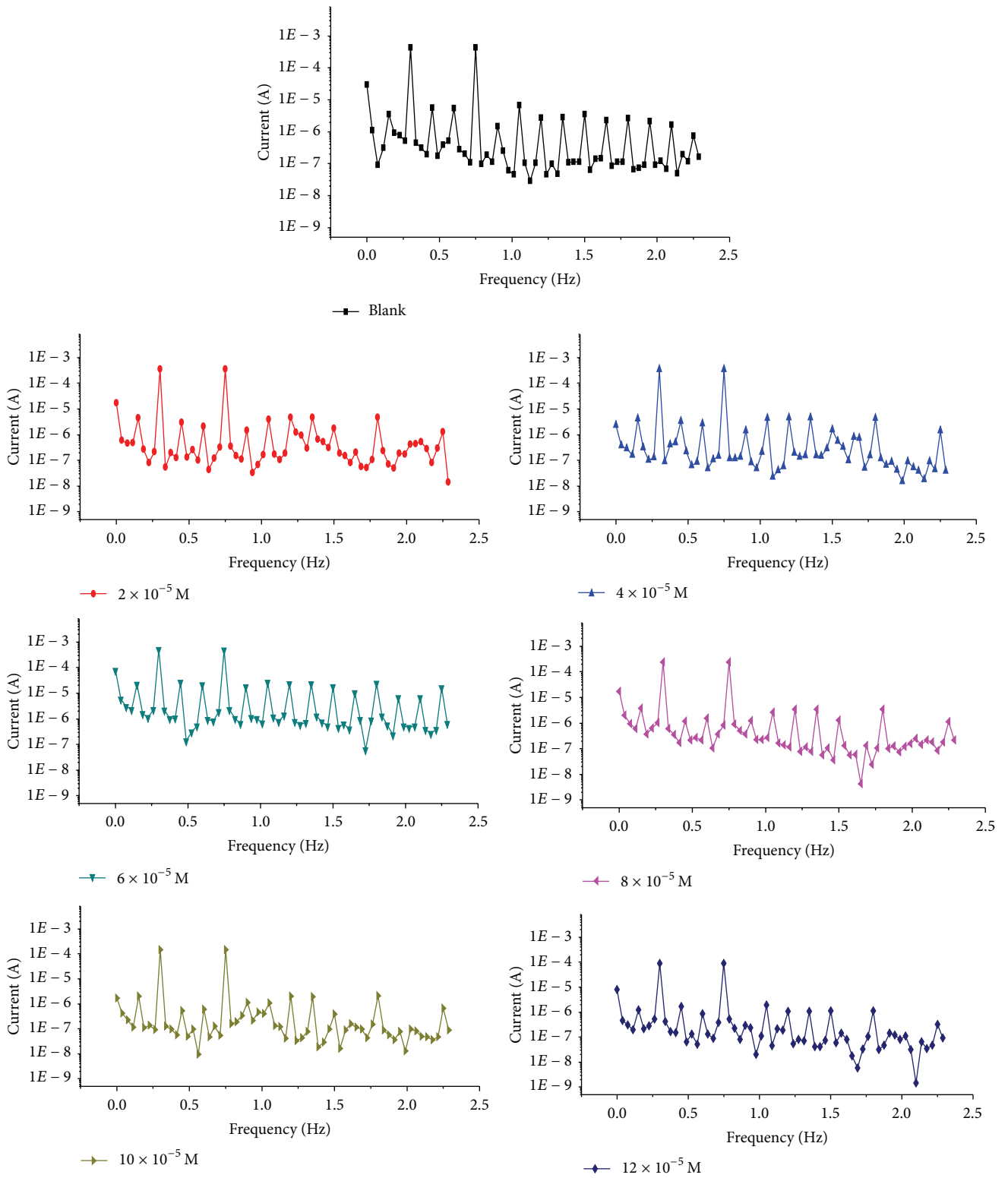


FIGURE 8: EFM spectra for carbon steel in 1 M HCl in the absence and presence of different concentrations of compound (A).

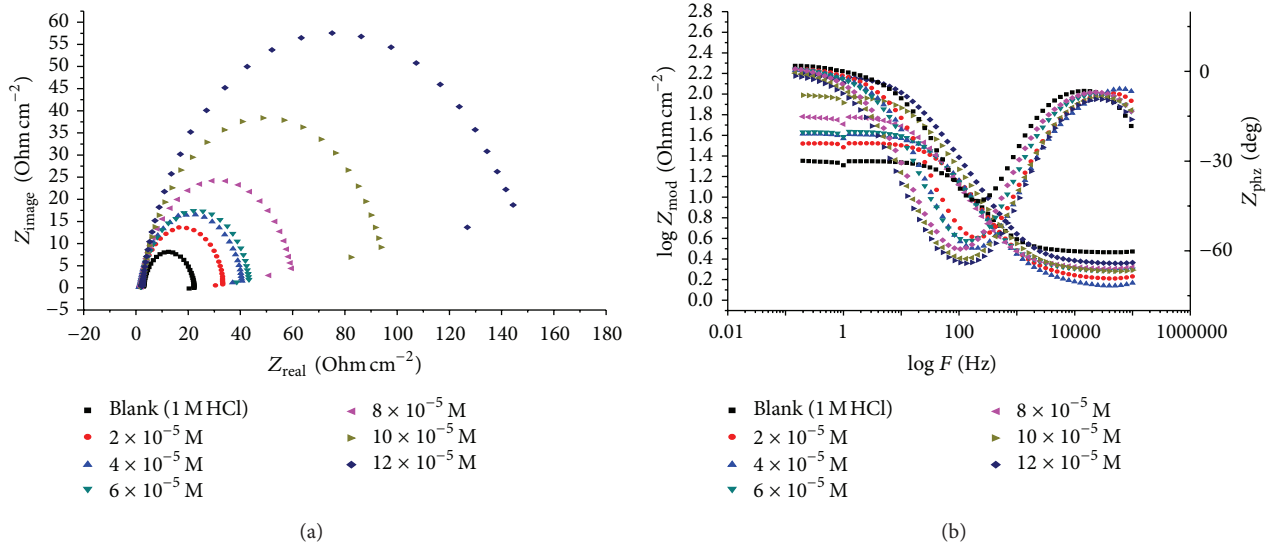


FIGURE 9: (a) The Nyquist plots for the corrosion of carbon steel in 1 M HCl in the absence and presence of different concentrations of inhibitor (A) at 25°C; (b) the Bode plots for the corrosion of carbon steel in 1 M HCl in the absence and presence of different concentrations of inhibitor (A) at 25°C.

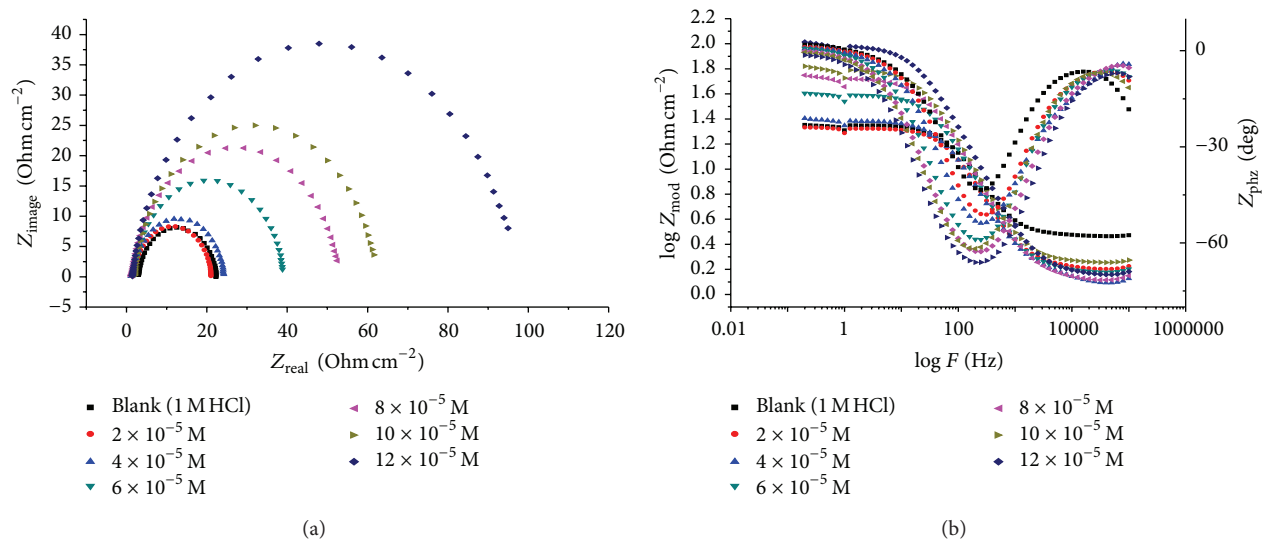


FIGURE 10: (a) The Nyquist plots for the corrosion of carbon steel in 1 M HCl in the absence and presence of different concentrations of inhibitor (B) at 25°C; (b) the Bode plots for the corrosion of carbon steel in 1 M HCl in the absence and presence of different concentrations of inhibitor (B) at 25°C.

Figure 8 shows the EFM intermodulation spectra (current versus frequency) of carbon steel in HCl solution containing different concentrations of compound (A). Similar curves were obtained for compounds (B and C) (not shown). The harmonic and intermodulation peaks are clearly visible and are much larger than the background noise. The two large peaks, with amplitude of about 200 μA , are the response to the 40 and 100 mHz (2 and 5 Hz) excitation frequencies. It is important to note that between the peaks there is nearly no current response (<100 nA). The experimental EFM data were treated using two different models: complete diffusion control of the cathodic reaction and the “activation” model.

For the latter, a set of three nonlinear equations had been solved, assuming that the corrosion potential does not change due to the polarization of the working electrode [38]. The larger peaks were used to calculate the corrosion current density (i_{corr}), the Tafel slopes (β_c and β_a), and the causality factors (CF-2 and CF-3). These electrochemical parameters were listed in Table 8. The data presented in Table 8 obviously show that the addition of any one of tested compounds at a given concentration to the acidic solution decreases the corrosion current density, indicating that these compounds inhibit the corrosion of carbon steel in 1 M HCl through adsorption. The causality factors obtained under different

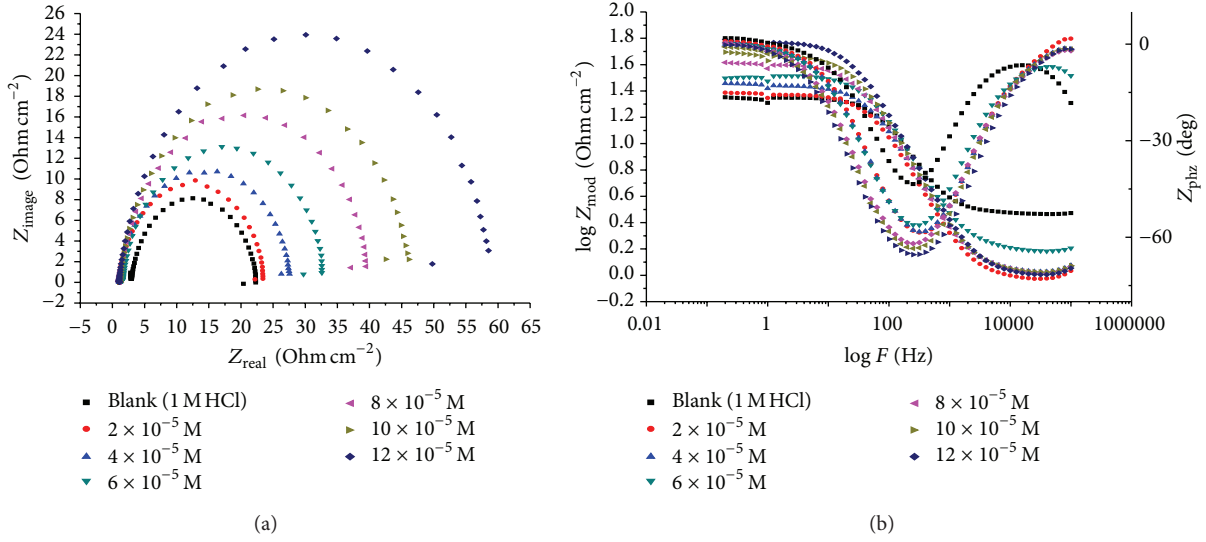


FIGURE 11: (a) The Nyquist plots for the corrosion of carbon steel in 1M HCl in the absence and presence of different concentrations of inhibitor (C) at 25°C; (b) the Bode plots for the corrosion of carbon steel in 1M HCl in the absence and presence of different concentrations of inhibitor (C) at 25°C.

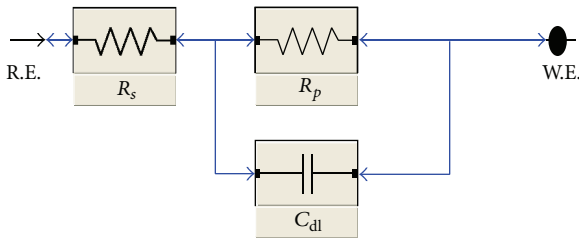


FIGURE 12: Equivalent circuit model used to fit experimental EIS.

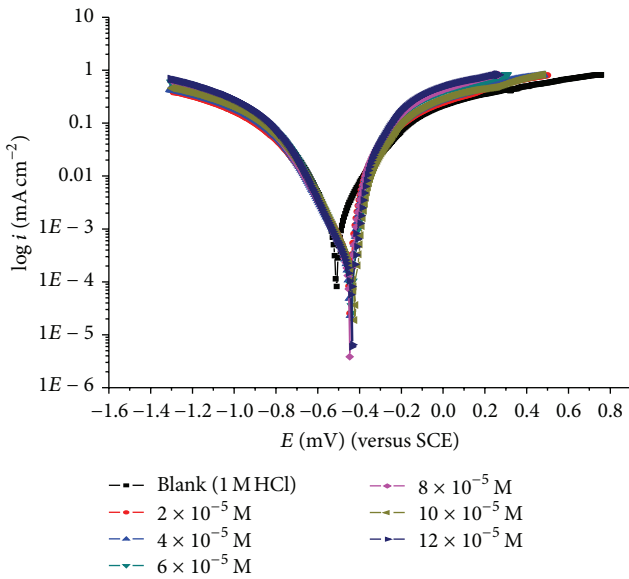


FIGURE 13: Potentiodynamic polarization curves for the dissolution of carbon steel in 1M HCl in the absence and presence of different concentrations of compound (A) at 25°C.

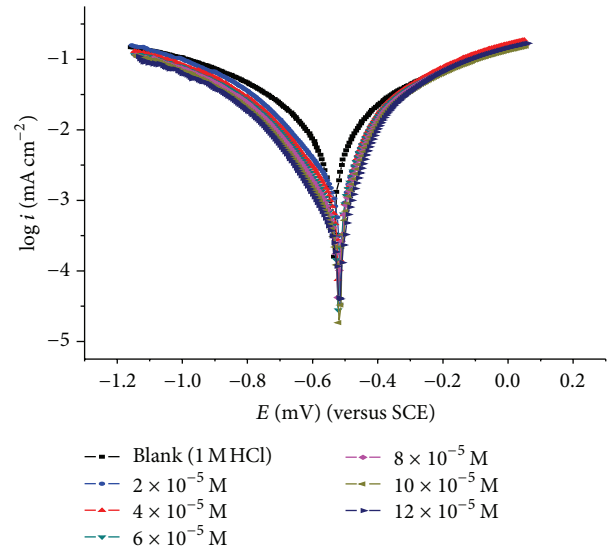


FIGURE 14: Potentiodynamic polarization curves for the dissolution of carbon steel in 1M HCl in the absence and presence of different concentrations of compound (B) at 25°C.

experimental conditions are approximately equal to the theoretical values (2 and 3) indicating that the measured data are verified and of good quality. The inhibition efficiencies $\%IE_{\text{EFM}}$ increase by increasing the inhibitor concentrations and were calculated as follows from (7):

$$\%IE_{\text{EFM}} = \left[1 - \left(\frac{i_{\text{corr}}}{i_{\text{corr}}^0} \right) \right] \times 100, \quad (7)$$

where i_{corr}^0 and i_{corr} are corrosion current densities in the absence and presence of inhibitor, respectively. The inhibition

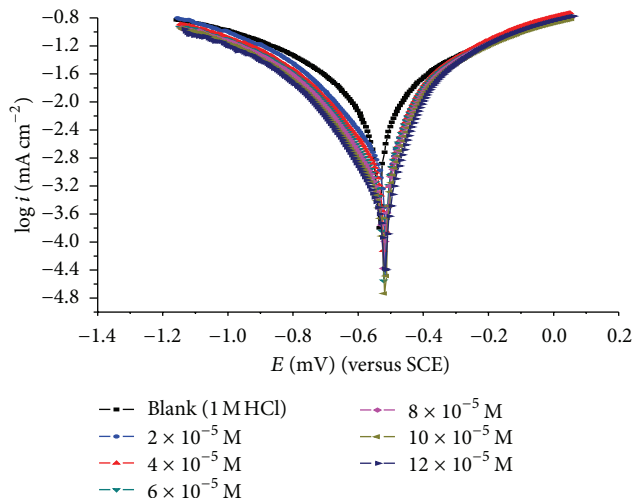


FIGURE 15: Potentiodynamic polarization curves for the dissolution of carbon steel in 1 M HCl in the absence and presence of different concentrations of compound (C) at 25°C.

sufficiency obtained from this method is in the the following order:

$$(A) > (B) > (C). \quad (8)$$

3.2.2. Electrochemical Impedance Spectroscopy (EIS). Impedance is a measure of the ability of a circle to resist the flow of electrical current. Electrochemical impedance is usually measured by applying an AC potential to an electrochemical cell and measuring the current through the cell. Surface properties, electrode kinetics, and mechanistic information can be obtained from impedance diagrams [39–43]. Figure 9 shows the Nyquist (a) and Bode (b) plots obtained at open-circuit potential both in the absence and presence of increasing concentrations of investigated compounds at 25°C. The increase in the size of the capacitive loop with the addition of investigated compounds shows that a barrier gradually forms on the carbon steel surface. The increase in the capacitive loop size (Figure 9(a)) is enhanced, at a fixed inhibitor concentration, following the order: (A) > (B) > (C), confirming the highest inhibitive influence of compound (A). Bode plots (Figure 9(b)) show that the total impedance increases with increasing inhibitor concentration ($\log Z$ versus $\log f$). But $\log f$ versus phase also Bode plot shows the continuous increase in the phase angle shift, obviously correlating with the increase of inhibitor adsorbed on carbon steel surface. The Nyquist plots do not yield perfect semicircles as expected from the theory of EIS. The deviation from ideal semicircle was generally attributed to the frequency dispersion [44] as well as to the inhomogeneities of the surface.

EIS spectra of the investigated compounds were analyzed using the equivalent circuit, Figure 12, which represents a single charge transfer reaction and fits well with our experimental results. The constant phase element, CPE, is introduced in the circuit instead of a pure double layer

capacitor to give a more accurate fit [45]. The double layer capacitance, C_{dl} , for a circuit including a CPE parameter (Y_0 and n) was calculated from [46]

$$C_{dl} = \frac{Y_0 \omega^{n-1}}{\sin [n(\pi/2)]}, \quad (9)$$

where Y_0 is the magnitude of the CPE, $\omega = 2\pi f_{max}$, f_{max} is the frequency at which the imaginary component of the impedance is maximal, and the factor n is an adjustable parameter that usually lies between 0.50 and 1.0. From Nyquist plots (Figures 9, 10, and 11), it was clear that the curves approximated by a single capacitive semicircles and showing that the corrosion process was mainly charged-transfer controlled [47, 48]. The general shape of the curves is very similar for all samples (in presence or absence of inhibitors at different immersion times) indicating that there is no change in the corrosion mechanism [49]. From the impedance data (Table 9), we concluded that the value of R_{ct} increases with increasing the concentration of the inhibitors and this indicates an increase in %IE_{EIS}, which is in concord with the EFM results obtained. In fact the presence of inhibitors enhances the value of R_{ct} in acidic solution. Values of double layer capacitance are also brought down to the maximum extent in the presence of inhibitor, and the decrease in the values of CPE follows the order similar to that obtained for i_{corr} in this study. The decrease in CPE/ C_{dl} results from a decrease in local dielectric constant and/or an increase in the thickness of the double layer, suggesting that organic derivatives inhibit the iron corrosion by adsorption at metal/acid [50, 51]. The inhibition efficiency was calculated from the charge transfer resistance data from (10) [52]:

$$\%IE_{EIS} = \left[1 - \left(\frac{R_{ct}^o}{R_{ct}} \right) \right] \times 100, \quad (10)$$

where R_{ct}^o and R_{ct} are the charge-transfer resistance values without and with inhibitor, respectively.

3.3. Potentiodynamic Polarization Measurements. Figures 13, 14, and 15 show the potentiodynamic polarization curves of carbon steel dissolution in 1 M HCl in the absence and presence of different concentrations of inhibitor (A, B, and C) at 25°C. The numerical values of the variation of the corrosion current density (i_{corr}), the corrosion potential (E_{corr}), Tafel slopes (β_a and β_c), the degree of surface coverage (θ), and the inhibition efficiency were recorded in Table 9. The inhibition efficiency and degree of surface coverage were calculated using

$$\%IE_p = \theta \times 100 = \left[\frac{(i_{corr}^o - i_{corr})}{i_{corr}^o} \right] \times 100, \quad (11)$$

where i_{corr}^o and i_{corr} are the uninhibited and inhibited corrosion current densities, respectively. The results of Table 9 indicate the following.

- (1) The cathodic and anodic curves obtained exhibit Tafel-type behavior. Addition of thiophene derivatives increased both the cathodic and anodic overvoltages and inhibited both the hydrogen evolution

TABLE 7: Activation parameters for carbon steel corrosion in the absence and presence of various concentrations of inhibitor (A) in 1 M HCl.

$C_{\text{inh.}} \times 10^{-5}$ (M)	Activation parameters		
	E_a^* (kJ mol ⁻¹)	ΔH^* (kJ mol ⁻¹)	ΔS^* (J mol ⁻¹ K ⁻¹)
Blank	58.50	24274.22	5574.8599
2	39.39	15975.93	1.5162
4	34.38	13798.83	0.1738
6	34.30	13764.91	0.1532
8	27.54	10830.32	0.0086
10	27.20	10682.49	0.0068
12	25.41	8712.32	0.0048

and the anodic dissolution processes that are mixed-type inhibitors.

- (2) The corrosion current density ($i_{\text{corr.}}$) decreases with increasing the concentration of the thiophene derivatives which indicates that these compounds act as inhibitors, and the degree of inhibition depends on the concentration and type of inhibitors present.
- (3) The slopes of anodic and cathodic Tafel lines (β_a and β_c) were slightly changed by increasing the concentration of the tested compounds. This indicates that these inhibitors act as mixed-type inhibitors. Tafel lines are parallel, which indicates that there is no change of the mechanism of inhibition in the presence and absence of inhibitors.
- (4) The orders of inhibition efficiency of all inhibitors at different concentrations as given by polarization measurements are listed in Table 9. The results are in good agreement with those obtained from weight loss measurements.

4. Mechanism

The inhibition mechanism involves the adsorption of the inhibitor on the metal surface immersed in aqueous HCl solution. Four types of adsorption [53] may take place involving organic molecules at the metal-solution interface:

- (1) electrostatic attraction between the charged molecules and the charged metal;
- (2) interaction of unshared electron pairs in the molecule with the metal;
- (3) interaction of π -electrons with the metal;
- (4) combination of all the above.

The fact that the adsorption of inhibitors on C-steel surface proceeded via chemical adsorption indicates that the mechanism is consistent with the transferred electron from

the inhibitor's molecule to the empty orbital of Fe in C-steel. In acid solution, the protonation of the inhibitors may occur easily, so it is difficult for the protonated compound to approach the positively charged carbon steel surface (H_3O^+ /metal interface) due to the electrostatic repulsion. Since chloride ions have a smaller degree of hydration; thus, they could bring excess negative charges in the vicinity of the interface and favour more adsorption of the positively charged inhibitor molecules and the protonated compounds adsorbed through electrostatic interactions between the positively charged molecules and the negatively charged metal surface. We hereby propose that the mechanism involves the protonation of the nitrogen to form NH_3^+ by HCl solution. Therefore, the cationic form of the inhibitors immersed in the acidic medium can compete with hydrogen proton (H^+) for the electrons on the metallic surface. Since the size of the inhibitor's cation is much larger than that of hydrogen molecule (due to the presence of the heterocyclic structures in the inhibitors), after the release of H_2 , the inhibitor returns to its neutral form with the electronegative group having a free electron pair that can facilitate its adsorption on C-steel surface. The adsorbed inhibitor can form complex with iron surface and then protect the metal against further corrosion attack by blocking its active sites by functional groups as C-S, C-O, N-H, O-H, and C=O and heterocyclic rings in their molecular structures. These functional groups have been reported in other literature as effective corrosion inhibitors [54, 55].

The results show that compound (A) exhibits better performance because it has 7 centers of adsorption (5N, 1S, and 1O), so that it cover a wide area of the metal surface and protect it, also the presence of $-\text{CH}_3$ group which acts as donating group increases the electron density on the active centers, that leads to increase coverage surface, thereby giving higher inhibition efficiency.

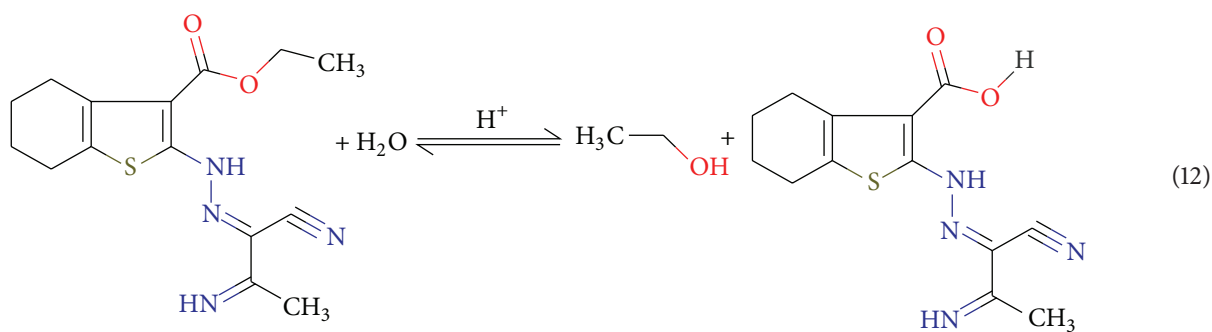
Compound (B) has also 7 centers of adsorption (4N, 1S, and 2O from ester group). Due to the existence of ester group which in the presence of acidic media converts to carboxylic group, which attack C-steel surface but with increase temperature the reversible reaction takes place [19] and the formed organic acid convert to ester again.

TABLE 8: Electrochemical kinetic parameters obtained from EFM technique for carbon steel in 1 M HCl in the absence and presence of different concentrations of compounds.

Compound	Concentration $\times 10^{-5}$ (M)	i_{corr} ($\mu\text{A cm}^{-2}$)	β_c (mV dec $^{-1}$)	β_a (mV dec $^{-1}$)	k_{corr} (mpy)	CF-2	CF-3	θ	%IE	
Blank	0	913.3	149	132	420.8	1.90	3.34	—	—	
	2	535.4	103	97	246.7	1.86	2.88	0.414	41.4	
	4	522.7	106	98	240.8	1.85	2.20	0.428	42.8	
	A	6	408.0	59	50	188.0	2.01	2.19	0.553	55.3
	8	338.7	97	92	156.0	1.37	2.37	0.629	62.9	
	10	222.7	100	97	102.6	1.88	2.60	0.756	75.6	
	12	138.9	110	97	64.0	1.88	2.42	0.848	84.8	
B	2	529.9	92	106	242.1	1.88	3.08	0.420	42.0	
	4	375.1	103	92	171.4	2.25	1.73	0.589	58.9	
	6	322.8	43	37	147.5	1.95	2.29	0.647	64.7	
	8	314.9	101	93	143.9	2.10	2.88	0.655	65.5	
	10	302.0	39	35	138.0	1.94	2.87	0.669	66.9	
	12	204.9	102	93	93.6	1.98	2.45	0.776	77.6	
C	2	503.1	101	90	229.9	1.86	2.88	0.449	44.9	
	4	433.5	102	94	198.1	1.85	2.20	0.525	52.5	
	6	341.1	98	88	155.9	2.01	2.19	0.627	62.7	
	8	337.1	101	95	154.0	1.37	2.37	0.631	63.1	
	10	307.5	54.0	78	140.5	1.88	2.60	0.663	66.3	
	12	288.8	102.6	93	131.9	1.88	2.42	0.684	68.4	

TABLE 9: Corrosion potential (E_{corr}), corrosion current density (i_{corr}), Tafel slopes (β_c , β_a), degree of surface coverage (θ), and inhibition efficiency (%IE $_p$) of carbon steel in 1 M HCl at 25°C for compounds A, B, and C.

Inhibitor	Concentration $\times 10^{-5}$ (M)	$-E_{\text{corr}}$ (mV)	i_{corr} ($\mu\text{A cm}^{-2}$)	β_c (mV dec $^{-1}$)	β_a (mV dec $^{-1}$)	k_{corr} (mpy)	θ	%IE $_p$	
1 M HCl	Blank	511	2170	206.7	205.3	992.3	—	—	
	2	449	695	199	111	317.6	0.680	68.0	
	4	447	543	195	118	248.1	0.750	75.0	
	A	6	438	458	183	99	209.1	0.789	78.9
	8	447	409	168	85	186.9	0.812	81.2	
	10	422	278	157	79	127.0	0.872	87.2	
	12	436	181	145	79	82.8	0.917	91.7	
B	2	507	1900	257	182	866.8	0.124	12.4	
	4	504	1130	188	136	516.3	0.479	47.9	
	6	497	800	189	154	365.6	0.631	63.1	
	8	486	453	188	133	207.1	0.791	79.1	
	10	482	310	140	105	141.5	0.857	85.7	
	12	472	205	162	108	93.9	0.906	90.6	
C	2	522	2050	211	188	936.6	0.055	5.5	
	4	526	1780	165	122	815.3	0.180	18.0	
	6	516	1200	167	125	549.2	0.447	44.7	
	8	474	455	171	119	196.9	0.790	79.0	
	10	491	387	130	85	176.8	0.822	82.2	
	12	478	310	140	97	141.7	0.857	85.7	



Compound (C) is less active than (A) and (B) because of its small molecular surface area (294.83), and *t* has 6 adsorption centers (5N and 1S). The presence of cyanide group (-CN) which acts as electron withdrawing group decreases the electron density on the active centers, which led to enhance the surface coverage, thereby giving lower inhibition efficiency.

5. Conclusions

From the results of the study the following may be concluded.

- (I) All the investigated compounds are good corrosion inhibitors for carbon steel in 1M HCl solution. The effectiveness of these inhibitors depends on their structures. The variation in inhibitive efficiency depends on the type and the nature of the substituent present in the inhibitor molecule.
- (II) Reasonably good agreement was observed between the values obtained by the weight loss and electrochemical measurements were in good agreement. The order of %IE of these investigated compounds is as follows: (A) > (B) > (C).
- (III) Results obtained from potentiodynamic polarization indicated that the investigated derivatives are mixed-type inhibitors.
- (IV) The thermodynamic parameters revealed that the inhibition of corrosion by investigated compounds is due to the formation of a chemisorbed film on the metal surface.
- (V) The adsorption of all investigated compounds onto steel surface follows the Langmuir adsorption isotherm model.

Conflict of Interests

The authors declare that there is no conflict of interests regarding the publication of this paper.

Acknowledgments

The authors are thankful to the Head of Chemistry Department, Mansoura University, and the Head of East Delta Electricity Production Company, Damietta, for their encouragement and necessary laboratory facilities.

References

- [1] M. Elayyachy, M. Elkodadi, A. Aouniti et al., "New bipyrazole derivatives as corrosion inhibitors for steel in hydrochloric acid solutions," *Materials Chemistry and Physics*, vol. 93, no. 2-3, pp. 281-285, 2005.
- [2] A. Popova, M. Christov, S. Raicheva, and E. Sokolova, "Adsorption and inhibitive properties of benzimidazole derivatives in acid mild steel corrosion," *Corrosion Science*, vol. 46, no. 6, pp. 1333-1350, 2004.
- [3] B. Mernari, H. Elatarri, M. Traisnel, F. Bentiss, and M. Lagrenee, "Inhibiting effects of 3,5-bis(n-pyridyl)-4-amino-1,2,4-triazoles on the corrosion for mild steel in 1 M HCl medium," *Corrosion Science*, vol. 40, no. 2-3, pp. 391-399, 1998.
- [4] X. Li, S. Deng, H. Fu, T. Li, and G. Mu, "Inhibition of the corrosion of cold rolled steel in hydrochloric acid solution by Tween-40," *Anti-Corrosion Methods and Materials*, vol. 56, no. 4, pp. 232-238, 2009.
- [5] Y. Sürme and A. A. Gürten, "Role of polyethylene glycol tert-octylphenyl ether on corrosion behaviour of mild steel in acidic solution," *Corrosion Engineering, Science and Technology*, vol. 44, no. 4, pp. 304-3011, 2009.
- [6] G. Y. Elewady, "Pyrimidine derivatives as corrosion inhibitors for carbon-steel in 2M hydrochloric acid solution," *International Journal of Electrochemical Science*, vol. 3, pp. 1149-1161, 2008.
- [7] I. Zaafarany and M. Abdallah, "Ethoxylated fatty amide as corrosion inhibitors for carbon steel in hydrochloric acid solution," *International Journal of Electrochemical Science*, vol. 5, no. 1, pp. 18-28, 2010.
- [8] A. Yurt, A. Balaban, S. U. Kandemir, and G. Bereket, "Investigation on some Schiff bases as HCl corrosion inhibitors for carbon steel," *Materials Chemistry and Physics*, vol. 85, no. 2-3, pp. 420-426, 2004.
- [9] S. A. Ali, H. A. Al-Muallema, S. U. Rahman, and M. T. Saeed, "Bis-isoxazolidines: a new class of corrosion inhibitors of mild steel in acidic media," *Corrosion Science*, vol. 50, no. 11, pp. 3070-3077, 2008.

- [10] H. Ju, Z. P. Kai, and Y. Li, "Aminic nitrogen-bearing polydentate Schiff base compounds as corrosion inhibitors for iron in acidic media: a quantum chemical calculation," *Corrosion Science*, vol. 50, no. 3, pp. 865–871, 2008.
- [11] D. I. Gopi, K. Govindaraju, and L. Kavhith, "Investigation of triazole derived Schiff bases as corrosion inhibitors for mild steel in hydrochloric acid medium," *Journal of Applied Electrochemistry*, vol. 40, no. 7, pp. 1349–1356, 2010.
- [12] M. A. Migahed, A. M. Abdul-Raheim, A. M. Atta, and W. Brostow, "Synthesis and evaluation of a new water soluble corrosion inhibitor from recycled poly(ethylene terephthalate)," *Materials Chemistry and Physics*, vol. 121, no. 1-2, pp. 208–214, 2010.
- [13] A. Singh and M. Quraish, "Inhibiting effects of 5-substituted isatin-based Mannich bases on the corrosion of mild steel in hydrochloric acid solution," *Journal of Applied Electrochemistry*, vol. 40, no. 7, pp. 1293–1306, 2010.
- [14] I. B. Obot, N. O. Obi-Egbedi, and N. W. Odozi, "Acenaphtho [1,2-b] quinoxaline as a novel corrosion inhibitor for mild steel in 0.5 M H₂SO₄," *Corrosion Science*, vol. 52, no. 3, pp. 923–926, 2010.
- [15] I. B. Obot and N. O. Obi-Egbedi, "Indeno-1-one [2,3-b]quinoxaline as an effective inhibitor for the corrosion of mild steel in 0.5 M H₂SO₄ solution," *Materials Chemistry and Physics*, vol. 122, no. 2-3, pp. 325–328, 2010.
- [16] H. Ashassi-Sorkhabi and M. Es'haghi, "Corrosion inhibition of mild steel in hydrochloric acid by betanin as a green inhibitor," *Journal of Solid State Electrochemistry*, vol. 13, no. 8, pp. 1297–1301, 2009.
- [17] F. M. Mahgoub, B. A. Abdel-Nabey, and Y. A. El-Samadisy, "Adopting a multipurpose inhibitor to control corrosion of ferrous alloys in cooling water systems," *Materials Chemistry and Physics*, vol. 120, no. 1, pp. 104–108, 2010.
- [18] B. I. Zerg, M. Sfair, M. Tale et al., "Effect of some tripodal bipyrazolic compounds on C38 steel corrosion in hydrochloric acid solution," *Journal of Applied Electrochemistry*, vol. 40, no. 9, pp. 1575–1582, 2010.
- [19] H. F. Eldien, *Synthesis of some new thiophenes with expected biological activity [M.S. thesis]*, Mansoura University, Mansoura, Egypt, 2012.
- [20] E. E. Oguzie, "Corrosion inhibition of mild steel in hydrochloric acid solution by methylene blue dye," *Materials Letters*, vol. 59, no. 8-9, pp. 1076–1079, 2005.
- [21] K. F. Khaled, "Application of electrochemical frequency modulation for monitoring corrosion and corrosion inhibition of iron by some indole derivatives in molar hydrochloric acid," *Materials Chemistry and Physics*, vol. 112, no. 1, pp. 290–300, 2008.
- [22] K. F. Khaled, "Evaluation of electrochemical frequency modulation as a new technique for monitoring corrosion and corrosion inhibition of carbon steel in perchloric acid using hydrazine carbodithioic acid derivatives," *Journal of Applied Electrochemistry*, vol. 39, no. 3, pp. 429–438, 2009.
- [23] R. W. Bosch, J. Hubrecht, W. F. Bogaerts, and B. C. Syrett, "Electrochemical frequency modulation: a new electrochemical technique for online corrosion monitoring," *Corrosion*, vol. 57, no. 1, pp. 60–70, 2001.
- [24] S. S. Abdel-Rehim, K. F. Khaled, and N. S. Abd-Elshafi, "Electrochemical frequency modulation as a new technique for monitoring corrosion inhibition of iron in acid media by new thiourea derivative," *Electrochimica Acta*, vol. 51, no. 16, pp. 3269–3277, 2006.
- [25] A. Yurt, G. Bereket, A. Kivrak, A. Balaban, and B. Erk, "Effect of Schiff bases containing pyridyl group as corrosion inhibitors for low carbon steel in 0.1 M HCl," *Journal of Applied Electrochemistry*, vol. 35, no. 10, pp. 1025–1032, 2005.
- [26] F. Bentiss, M. Traisnel, and M. Lagrenee, "The substituted 1,3,4-oxadiazoles: a new class of corrosion inhibitors of mild steel in acidic media," *Corrosion Science*, vol. 42, no. 1, pp. 127–146, 2000.
- [27] W. Durnie, R. de Marco, A. Jefferson, and B. Kinsella, "Development of a structure-activity relationship for oil field corrosion inhibitors," *Journal of the Electrochemical Society*, vol. 146, no. 5, pp. 1751–1756, 1999.
- [28] G. Banerjee and S. N. Malhotra, "Contribution to adsorption of aromatic amines on mild steel surface from HCl solutions by impedance, UV, and Raman spectroscopy," *Corrosion*, vol. 48, no. 1, pp. 10–15, 1992.
- [29] E. S. Ivanov, *Inhibitors for Metal Corrosion in Acid Media*, Metallurgy, Moscow, Russia, 1986.
- [30] F. Bentiss, M. Lebrini, and M. Lagrenee, "Thermodynamic characterization of metal dissolution and inhibitor adsorption processes in mild steel/2,5-bis(n-thienyl)-1,3,4-thiadiazoles/hydrochloric acid system," *Corrosion Science*, vol. 47, no. 12, pp. 2915–2931, 2005.
- [31] M. Lebrini, F. Bentiss, H. Vezin, and M. Lagrenee, "The inhibition of mild steel corrosion in acidic solutions by 2,5-bis(4-pyridyl)-1,3,4-thiadiazole: structure-activity correlation," *Corrosion Science*, vol. 48, no. 5, pp. 1279–1291, 2006.
- [32] M. Bouklah, B. Hammouti, M. Lagrenee, and F. Bentiss, "Thermodynamic properties of 2,5-bis(4-methoxyphenyl)-1,3,4-oxadiazole as a corrosion inhibitor for mild steel in normal sulfuric acid medium," *Corrosion Science*, vol. 48, no. 9, pp. 2831–2842, 2006.
- [33] T. P. Hour and R. D. Holliday, "The inhibition by quinolines and thioureas of the acid dissolution of mild steel," *Journal of Applied Chemistry*, vol. 3, no. 11, pp. 502–513, 1953.
- [34] L. O. Riggs Jr. and T. J. Hurd, "Temperature coefficient of corrosion inhibition," *Corrosion*, vol. 23, no. 8, pp. 252–260, 1967.
- [35] G. M. Schmid and H. J. Huang, "Spectro-electrochemical studies of the inhibition effect of 4,7-diphenyl-1,10-phenanthroline on the corrosion of 304 stainless steel," *Corrosion Science*, vol. 20, no. 8-9, pp. 1041–1057, 1980.
- [36] J. Marsh, *Advanced Organic Chemistry*, Wiley Eastern, New Delhi, India, 3rd edition, 1988.
- [37] E. Kus and F. Mansfeld, "An evaluation of the electrochemical frequency modulation (EFM) technique," *Corrosion Science*, vol. 48, no. 4, pp. 965–979, 2006.
- [38] G. A. Caignan, S. K. Metcalf, and E. M. Holt, "Thiophene substituted dihydropyridines," *Journal of Chemical Crystallography*, vol. 30, no. 6, pp. 415–422, 2000.
- [39] D. C. Silverman and J. E. Carrico, "Electrochemical impedance technique—a practical tool for corrosion prediction," *Corrosion*, vol. 44, no. 5, pp. 280–287, 1988.
- [40] W. J. Lorenz, "Determination of corrosion rates by electrochemical DC and AC methods," *Corrosion Science*, vol. 21, no. 9-10, pp. 647–672, 1981.
- [41] D. D. Macdonald and M. C. Mckubre, "Impedance measurements in Electrochemical systems," in *Modern Aspects of Electrochemistry*, J. O. M. Bockris, B. E. Conway, and R. E. White, Eds., vol. 14, p. 61, Plenum Press, New York, NY, USA, 1982.

- [42] F. Mansfeld, "Recording and analysis of AC impedance data for corrosion studies," *Corrosion*, vol. 37, no. 5, pp. 301–307, 1981.
- [43] C. Gabrielli, Identification of Electrochemical processes by Frequency Response Analysis, Solartron Instrumentation Group, 1980.
- [44] M. El Achouri, S. Kertit, H. M. Goultaya et al., "Corrosion inhibition of iron in 1 M HCl by some gemini surfactants in the series of alkanediyl- α,ω -bis-(dimethyl tetradecyl ammonium bromide)," *Progress in Organic Coatings*, vol. 43, no. 4, pp. 267–273, 2001.
- [45] J. R. Macdonald and W. B. Johanson, *Theory in Impedance Spectroscopy*, John Wiley & Sons, New York, NY, USA, 1987.
- [46] S. F. Mertens, C. Xhoffer, B. C. de Cooman, and E. Temmerman, "Short-term deterioration of polymer-coated 55% Al-Zn. Part 1. Behavior of thin polymer films," *Corrosion*, vol. 53, no. 5, pp. 381–387, 1997.
- [47] G. TrabANELLI, C. Montecelli, V. Grassi, and A. Frignani, "Electrochemical study on inhibitors of rebar corrosion in carbonated concrete," *Cement and Concrete Research*, vol. 35, pp. 1804–1813, 2005.
- [48] A. J. Trowsdate, B. Noble, S. J. Haris, I. S. R. Gibbins, G. E. Thomson, and G. C. Wood, "The influence of silicon carbide reinforcement on the pitting behaviour of aluminium," *Corrosion Science*, vol. 38, no. 2, pp. 177–191, 1996.
- [49] F. M. Reis, H. G. de Melo, and I. Costa, "EIS investigation on Al 5052 alloy surface preparation for self-assembling monolayer," *Electrochimica Acta*, vol. 51, no. 8-9, pp. 1780–1788, 2006.
- [50] M. Lagrenée, B. Mernari, M. Bouanis, M. Traisnel, and F. Bentiss, "Study of the mechanism and inhibiting efficiency of 3,5-bis(4-methylthiophenyl)-4H-1,2,4-triazole on mild steel corrosion in acidic media," *Corrosion Science*, vol. 44, no. 3, pp. 573–588, 2002.
- [51] E. McCafferty and N. Hackerman, "Double layer capacitance of iron and corrosion inhibition with polymethylene diamines," *Journal of The Electrochemical Society*, vol. 119, pp. 146–154, 1972.
- [52] H. Ma, S. Chen, L. Niu, S. Zhao, S. Li, and D. Li, "Inhibition of copper corrosion by several Schiff bases in aerated halide solutions," *Journal of Applied Electrochemistry*, vol. 32, no. 1, pp. 65–72, 2002.
- [53] D. P. Schweinsberg, G. A. George, A. K. Nanayakkara, and D. A. Steinert, "The protective action of epoxy resins and curing agents-inhibitive effects on the aqueous acid corrosion of iron and steel," *Corrosion Science*, vol. 28, no. 1, pp. 33–42, 1988.
- [54] M. Shyamala and P. K. Kasthuri, "The inhibitory action of the extracts of *Adathoda vasica*, *Eclipta alba*, and *Centella asiatica* on the corrosion of mild steel in hydrochloric acid medium: a comparative study," *International Journal of Corrosion*, vol. 2012, Article ID 852827, 13 pages, 2012.
- [55] I. E. Uwah, P. C. Okafor, and V. E. Ebiekpe, "Inhibitive action of ethanol extracts from *Nauclea latifolia* on the corrosion of mild steel in H₂SO₄ solutions and their adsorption characteristics," *Arabian Journal of Chemistry*, vol. 6, no. 3, pp. 285–293, 2013.



Hindawi

Submit your manuscripts at
<http://www.hindawi.com>

